Anette Eltner, Dirk Hoffmeister, Andreas Kaiser, Pierre Karrasch,
Lasse Klingbeil, Claudia Stöcker, Alessio Rovere (eds.)

UAVs for the Environmental Sciences

Methods and Applications

wbg Academic

Die Deutsche Nationalbibliothek verzeichnet diese Publikation
in der Deutschen Nationalbibliographie; detaillierte bibliographische
Daten sind im Internet über www.dnb.de abrufbar

wbg Academic ist ein Imprint der wbg

Die Herausgabe des Werkes wurde durch die
Vereinsmitglieder der wbg ermöglicht.
Satz und eBook: Satzweiss.com Print, Web, Software GmbH
Umschlagsabbildungsnachweis:
Front 1 – Outcrop of Last Interglacial (125.000 years ago) limestones in the Seychelles. Image credits Alessio Rovere.
Front 2 – UAV hovering over a corn field in Bonn, Germany. Image credits Volker Lannert.
Front 3 – River mapping in a Boreal forest in Northern Finland. Image credits Eliisa Lotsari.
Back 1 – Dislocated boulders at a shoreline near Elaphonisos, Greece. Image credits Dirk Hoffmeister.
Back 2 – UAV in front of the Turtmann Glacier in Valais, Switzerland. Image credits Jana Eichel.
Back 3 – Sunken ancient bridge in a temporary empty water dam in Eastern Germany. Image credits Anette Eltner.
Gedruckt auf säurefreiem und
alterungsbeständigem Papier
Printed in Germany

Besuchen Sie uns im Internet: www.wbg-wissenverbindet.de

ISBN 978-3-534-40588-6

Elektronisch ist folgende Ausgabe erhältlich:
eBook (PDF): 978-3-534-40590-9

2.4 Thermal-infrared imaging

Emile Faye, Audrey Jolivot, Jérôme Théau, Jean-Luc Regnard, David Gómez-Candón

Infrared thermography is a non-invasive method that uses a thermal imager (thermal camera) to detect radiation (heat) emitted by all objects above absolute zero temperature and converting it into temperature. Thermal cameras provide a continuous distribution of surface temperature, called thermogram, that makes possible to detect heat-producing objects invisible to the hu-

man eye (Vollmer & Möllmann, 2010). Major developments in infrared thermography over the past decade significantly improved its application in various domains: military (guidance systems and engine detection), electronic (detecting overloaded electrical circuits), surveillance, research and rescue of people, disease control (Covid-19 fever), wildlife survey (animal detection), medical (assessment of circulatory disorders), building inspection (heat losses), etc. Among these applications, infrared thermography has also been increasingly used in various fields of environmental sciences such as animal (Briscoe et al., 2014) and plant physiology (Still et al., 2019), agronomy (Maes & Steppe, 2012) and landscape ecology (Scherrer & Koerner, 2010).

Thermal cameras embarked onboard UAVs can harvest thermal-infrared (TIR) images remotely, providing low-cost approaches to meet the critical requirements of bridging fine spatial and temporal resolutions with the covering of large environmental scenes. Autonomously operated, flying low and slow, UAVs equipped with TIR cameras offer scientists new opportunities for measuring and studying thermal environments. By this mean, the spatial variability of temperature across an ecosystem or at the organism level (e.g., plant) can be acquired over large areas and at a greater level of detail (Figure 2.4-1) compared to ground-based thermal imagery or usual recording with temperature loggers. In addition, the price of TIR cameras and UAVs are continuously decreasing, while their management and maintenance become more automatic and simpler. Consequently, these flying systems are currently becoming more affordable and accessible.

However, recording appropriate thermal data using TIR cameras onboard UAVs is not straightforward, as many pitfalls must be bypassed along the acquisition process. Indeed, depending on the objectives of the study to be addressed, either to retrieve the accurate surface temperature of an object of interest (Gómez-Candón et al., 2016), or to map and compare the thermal heterogeneities at the landscape scale (Faye et al., 2016a), or simply to detect endothermic animals (Chrétien et al.,2016; Burke et al., 2019), the use of TIR cameras onboard UAVs raises some major issues that have to be taken into consideration before flying.

For instance, TIR imaging devices that meet the constraints of weight and energy consumption of UAVs are based on microbolometric sensors that are not stabilized at a constant temperature, resulting in instability and drift in the temperature recording. Moreover, the spatial resolution of the TIR sensors restricts the flight planning for thermal mapping and makes the mosaicking of TIR images less accurate in the photogrammetry process than for Red Green Blue (RGB) images. Temperature measurements performed by TIR cameras are also affected by the physical properties of the studied object such as his capacity to emit in the thermal band (i.e., the object emissivity). The ratio between object size and the spatial resolution of the image, the thermal contrast between the target and its environment also impact TIR measurements. Several parameters external to the studied object affect the values recorded by the thermal sensors such as the ambient atmospheric conditions (e.g., air temperature and humidity, atmospheric pres-

sure, wind speed) and the presence of fog, dust or smoke (Meier et al., 2011). Varying weather conditions during the acquisition flight (e.g., cloud passes) will also have strong impacts on TIR readings. In studies requiring accurate temperature measurements, these effects must be minimized and corrected using a proper radiometric calibration, which requires the acquisition of meteorological data.

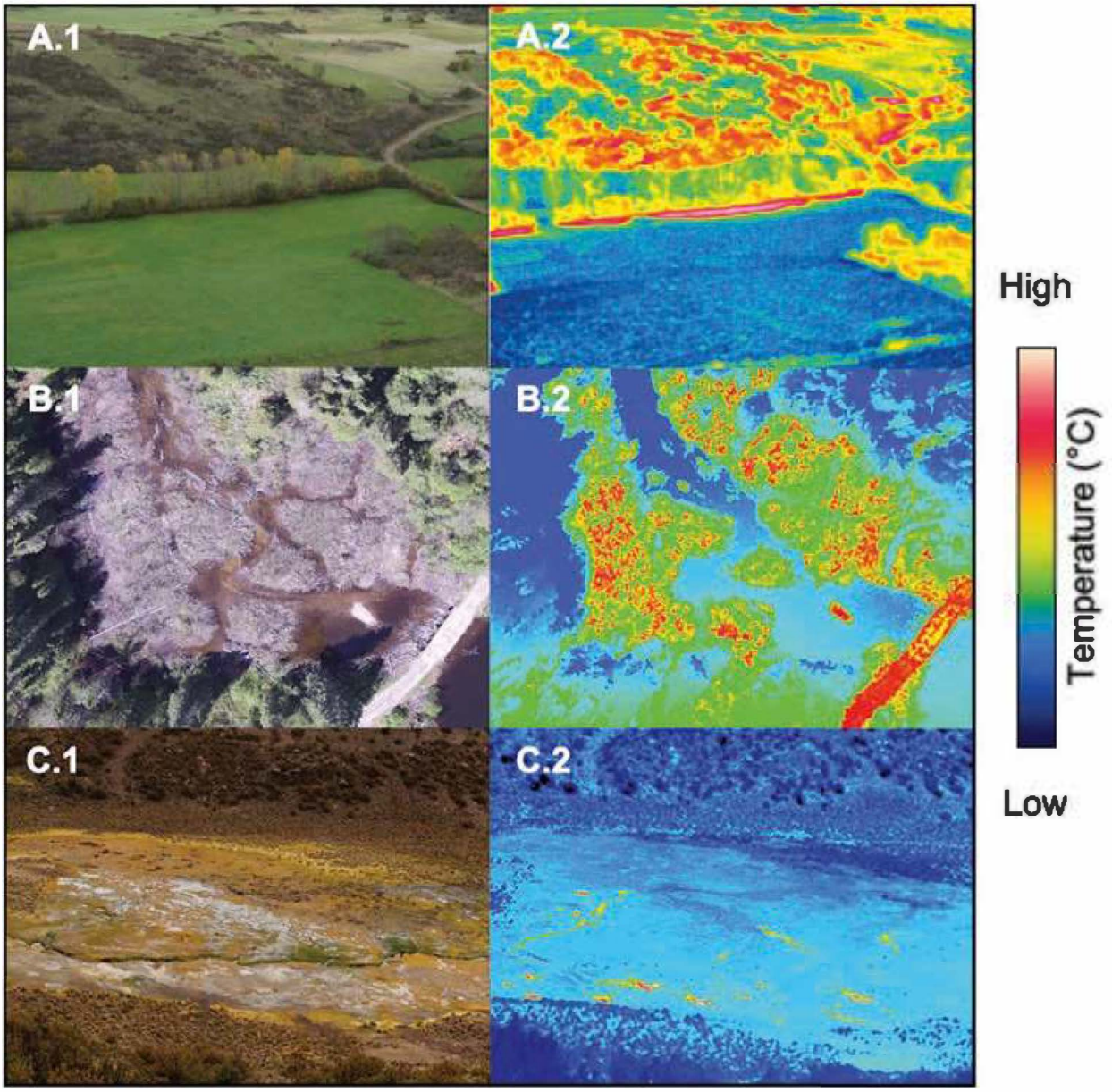

Figure 2.4-1: Examples of thermal-infrared images captured on-board UAVs for addressing environmental issues. 1 and 2 show the RGB and TIR images, respectively. (A) Agroecological landscape in the center of France. (B) Riparian and stream ecosystem in Quebec, Canada. (C) Hot springs in the Sajama altiplano, Bolivia. (A) and (C) © CIRAD – E. Faye. (B) © Centre de géomatique du Québec – P. Ménard. All rights reserved.

This chapter details the TIR cameras functioning and settings, specificities of TIR flight planning, radiometric calibrations and geometric corrections, meteorological recording, orthomosaicking of TIR images, and illustrated TIR data analysis from object-based and thermal landscape analysis to vegetation indices. Finally, we illustrate some of the challenges and limits of using TIR cameras onboard UAVs that remain to be overcome in the future.

2.4.1 Principles and functioning of thermal imaging

2.4.1.1 The theory of thermal-infrared

Infrared thermography is an imaging method that records the radiation emitted by an object at wavelengths ranging from 7.5 to 14 μm in the electromagnetic spectrum. Object radiates in the thermal-infrared band as a result of the molecular motion that relies on its temperature [1]: the hotter the object, the more its molecules move, the more the object emits in the thermal-infrared. According to the Planck's law, the radiations emitted by a perfect blackbody (i.e., a theoretical object at thermal equilibrium that absorbs all radiations) will depend only on its temperature, whatever its composition or shape (see [1] for details). Under the same conditions, any real object will emit radiation as a proportion of the blackbody radiation. This ratio is characterized by the emissivity of the object (ε) that illustrates its effectiveness to emit TIR radiations. Emissivity values varies between zero and one depending on the chemical composition and physical structure of the object. For instance, the emissivity of plants ranges between 0.95 and 0.99, higher when they contain more chlorophyll and water, with an average of 0.98 meaning that their surface emits 98 % of the energy emitted by a perfect blackbody at the same temperature (Rubio, 1997). Consequently, any object that has a temperature above the absolute zero (-273.15°C or 0 K at which all molecular motion stops) will emit a define quantity of radiations in the TIR band depending on its temperature and emissivity.

2.4.1.2 How thermal-infrared cameras work?

TIR cameras are imaging devices that deliver a visual representation of the thermal radiation emitted by objects. Because of their low load capacity, UAVs need to carry light-weight, small size, low power, and uncooled thermal cameras, in where the TIR sensor is not stabilized to a constant temperature (Kelly et al., 2019). The functioning of uncooled TIR cameras is based on a microbolometer sensor (Figure 2.4-2) made of an array of pixels built in an absorbing material that has a temperature-dependent electrical resistance (commonly silicon or vanadium).

When TIR radiations heat the detector material, the electrical signal variation is measured and compared to the value at the operating temperature of the sensor. By taking into account the ambient temperature and object emissivity, these changes in electrical signals are converted into temperature values that are displayed as monochrome or false-color images (i.e., 1 band), visible by human eyes.

One major difference with optical RGB cameras is that the lenses of TIR cameras cannot be made of glass, as glass blocks the TIR radiations. Thus, lenses are made of specific materials (such as crystalline silicon or fluoride) that is one of the main reasons explaining the high cost of TIR cameras (between 1000 to 10,000 US dollars). Another specificity of using uncooled TIR cameras is the lack of internal temperature control system (conversely to cooled TIR cameras) that bring instability and strong drift in temperature acquisition by the microbolometers (Mesas-Carrascosa et al., 2018). In order to reduce this drift during operation, and consequently to reduce the inaccuracies in temperature measurements, uncooled TIR cameras are equipped with a self-calibration system taking advantage of an internal reference source that regularly updates the offset parameters (Olbrycht et al., 2012). This self-calibration harmonizes the response signal across the entire sensor and reduces the inaccuracies due to the sensor temperature dependency (Mesas-Carrascosa et al., 2018). The TIR camera inconveniences must be taken into account to retrieve accurate surface temperatures (see 2.4.3.).

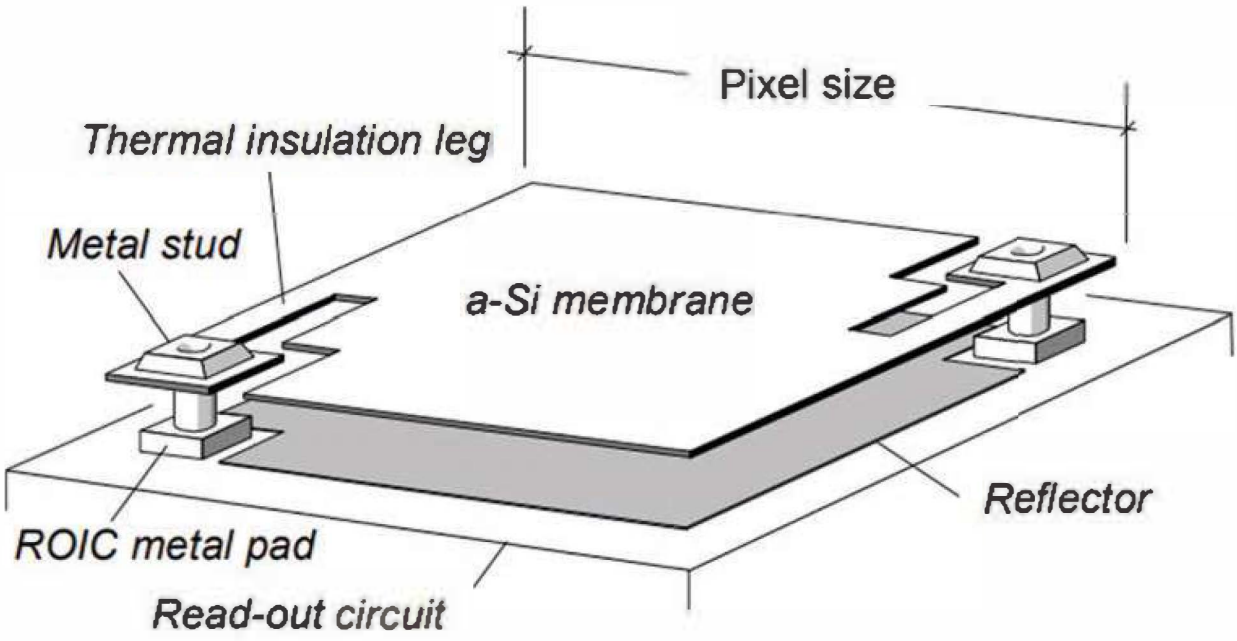

Figure 2.4-2: Schematic of a silicon-based microbolometer pixel. Reproduced with permission from SPIE – the International Society for Optics and Photonics: Yon et al., 2008.

2.4.1.3 Which TIR cameras are available for UAVs?

Choosing a TIR camera for UAV applications depends on the spatial resolution and thermal accuracy needed, but also the weight and the price of the device. Due to their building properties, the sensors of uncooled TIR cameras offer a much lower **spatial resolution** (mostly 640 x 480 pixels, Table 2.4-1) than other cameras suitable to be carried onboard UAVs, although most expensive cameras can achieve a resolution of 1,280 x 1,024 pixels. The low resolution of the TIR sensors brings issues for TIR acquisition that has to be considered. The UAV flights must be planned in stable atmospheric conditions (e.g., no clouds, low wind speed) while the resolution of thermal image (depending on the flight altitude) must be fine enough to avoid an excess of mixed pixels at the border of objects of interest. Moreover, the thermal sensitivity, or noise-equivalent temperature difference expressed in milli-Kelvin, is another key parameter for choosing a TIR camera. **Thermal sensitivity** (or thermal resolution) measures for how well a TIR camera is able to distinguish between very small differences in thermal radiation within one image. Manufacturers also provide temperature accuracies for their TIR cameras that represents the error made by the camera on temperature reading. **Thermal accuracy** usually ranges between ±0.1 and ±5°C. However, numerous studies have shown that the accuracy of the TIR camera depends on the ambient conditions in which the shooting occurs. For instance, Kelly et al. (2019) revealed that the thermal accuracy of a Flir Vue Pro (radiometrically uncalibrated, FLIR Systems, Inc., Wilsonville, USA) varied from ±0.5°C when used under stable laboratory conditions (i.e., air temperature maintained constant at 20.6°C) to ±5°C when used in outdoor conditions for TIR UAV mapping (with flight conditions varying between partly cloudy to full sun, air temperatures between 20–28°C, and wind speeds up to 4 ms^{-1}). Finally, some TIR cameras are factory-calibrated to generate non-uniformity compensation coefficients which are applied automatically by the camera in real time to maintain good image quality. These coefficients are based on pre-set ambient temperature, shooting distance, and take into account the TIR radiations emitted by the different parts of the camera itself (Olbrycht et al., 2012) (e.g., interior, lens).

Table 2.4-1: Examples of currently available thermal cameras to be carried onboard UAVs.

Camera model	Spatial Resolution (px)	Weight (g)	Spectral band (µm)	Thermal accuracy (°C)	Internal calibration
Micasense Altum*	160 x 120	357	8.0–14.0	+/- 5	Radiometric
FLIR Duo Pro R**	640 x 512	325	7.5–13.5	+/- 5	Radiometric
FLIR Vue Pro R	640 x 512	114	7.5–13.5	+/- 5	Radiometric
FLIR Tau 2 640	640 x 512	265	7.5–13.5	+/- 2	Uncalibrated
Thermoteknix MicroCAM 3	640 x 480	107	8.0–12.0	+/- 2	Uncalibrated
Gobi-640	640 x 480	263	8.0–14.0	+/- 2	Radiometric
ICI 9640 P-Series	640 x 480	137	7.0–14.0	+/- 2	Radiometric
InfraTec VarioCAM HD 600	640 x 480	1,150	7.5–14.0	+/- 1	Radiometric
Optris PI 640	640 x 480	320	7.5–13.0	+/- 2	Radiometric
Pearleye P-030 LWIR	640 x 480	760	8.0–14.0	+/- 2	NA
Tamarisk 640	640 x 480	121	8.0–14.0	+/- 2	NA
Thermal-Eye 4500AS	640 x 480	108	7.0–14.0	+/- 2	NA

* Combined with a 5-band sensor (R, G, B, red edge, near-infrared)
** Combined with a 4K RGB camera

2.4.2 Acquisition processes with TIR UAV

Before taking off with a TIR camera onboard a UAV, many particularities must be taken into account in order to accurately retrieve both accurate or relative surface temperatures, such as TIR camera settings, flight planning, weather conditions, geometric and radiometric corrections, and orthomosaicking. Below, we present a step-by-step process to follow for obtaining high-resolution spatially distributed correct temperatures that can be used to address environmental issues (Figure 2.4-3).

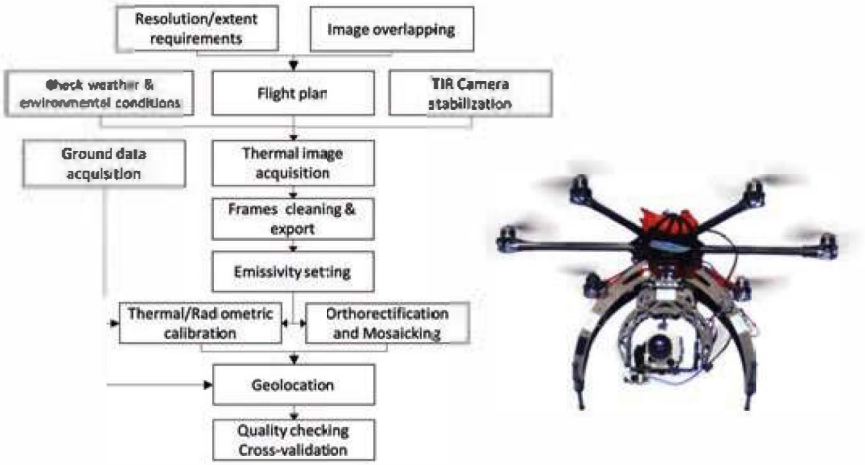

Figure 2.4-3: An example of a methodological flowchart to acquire and process thermal-infrared images with UAV. Photograph of an uncooled TIR camera (InfraTec VarioCAM® HR 600) onboard a flying platform © CIRAD – E. Faye. All rights reserved.

2.4.2.1 The flying platform

Depending on the applications, different types of UAVs can carry TIR cameras onboard (Watts et al., 2012). In most cases, TIR cameras will be embarked on UAV multi-copters that provide more stability and can hover. As always, flying an UAV is a trade-off between the payload, the battery capacity, the flight elevation and speed, the extent covered, and the desired image resolution. Flying with TIR cameras onboard will affect each of these parameters. Indeed, the flight time significantly decreases as the payload increases. TIR camera made for UAV applications are usually connected, managed and thus fully interoperable with the UAV system and flight controller: control, tilting, and triggering are based on the Global Navigation Satellite System (GNSS) data of the platform.

2.4.2.2 Ground measurement devices

The thermal radiance emitted by the object and captured by the TIR camera is modified by the qualitative and quantitative features of the atmosphere between the object and the sensor (Scherer & Koerner, 2010). Indeed, the atmosphere: (i) reduces the original signal (by absorption and scattering), and (ii) adds its own signal (related to the atmosphere temperature, its relative humidity and other components). This results in a change in the TIR readings by the camera as the shooting distance increases (Figure 2.4-4), even at very low distance (Faye et al., 2016b).

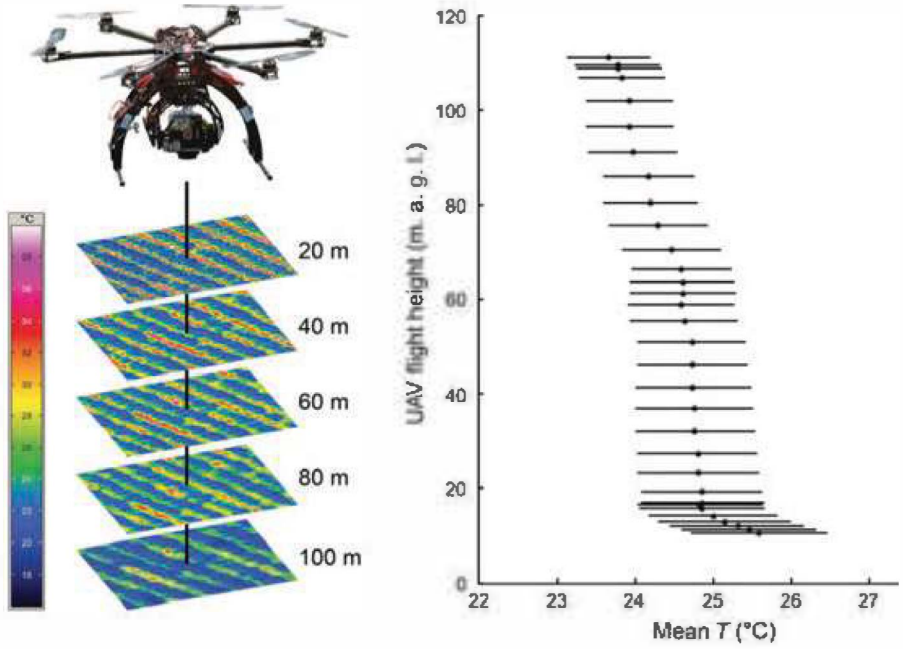

Figure 2.4-4: Effect of flight height on TIR readings (adapted from Faye et al., 2016a with permission of Wiley).

In order to retrieve an accurate and absolute measurement of the surface temperature of the object of interest, various methods have been described in the literature: application of radiative transfer models (i.e., simulating atmospheric interference, Dubuisson et al. (2005)), empirical atmospheric radiance corrections using ambient temperature of a blackbody (linear or polynomial models, Torres-Rua (2017)), or neural networks (Ribeiro-Gomes et al., 2017). In practice, using an empirical calibration method based on known temperatures of thermal targets on the ground to apply the radiometric correction on the TIR images is the most commonly used method (Kelly et al., 2019). This is the method presented below.

- Radiometric thermal targets
  The radiometric correction detailed here is based on the knowledge of the absolute surface temperature of specific objects (radiometric thermal targets) during the airborne TIR image acquisition. The device is composed of four contrasted temperature targets (Lambertian surfaces) that produce a large temperature range: two extreme temperature targets, that represent the hottest and coolest temperature of the area of interest, and two intermediate temperature targets. For example, targets can be made of: white polystyrene (cold), black-painted wood panel (hot), and dry and wet bare soil for intermediate targets (Figure 2.4-5). The temperatures of each target can be continuously measured during the UAV flight using thermo-radiometers

placed above the target (such as IR120, Campbell Scientific, ±0.2°C accuracy when calibrated against a blackbody) and recorded by a datalogger (Jolivot et al., 2017). Alternatively, temperature of ground targets can be measured continuously using a thermocouple placed at the surface of the targets. Radiometric targets must be located within the cover zone of the UAV flight and be large enough to ensure they are easily detectable within the UAV images (i.e., several homogenous pixels in the TIR image depending on the resolution of the TIR camera used).

- Geometric thermal targets
  Similar to RGB mapping, thermal ground control points (TGCPs) improve the georeferencing of TIR mapping products. TGCPs must be easily identifiable in the TIR bands. Indeed, not all objects appearing in an RGB image might be distinguishable in the TIR image. For example, two features of different colours (different signature in the visible spectrum) can have the same temperature and become not distinguishable in TIR images, and vice-versa (can you spot the cold stream in Figure 2.4-1C.2). It is therefore advisable to use high or low reflective surfaces displaying a high thermal contrast with the surroundings (Figure 2.4-6). Different materials and shapes are suitable to make easily recognisable TGCPs (e.g., cross, tri-

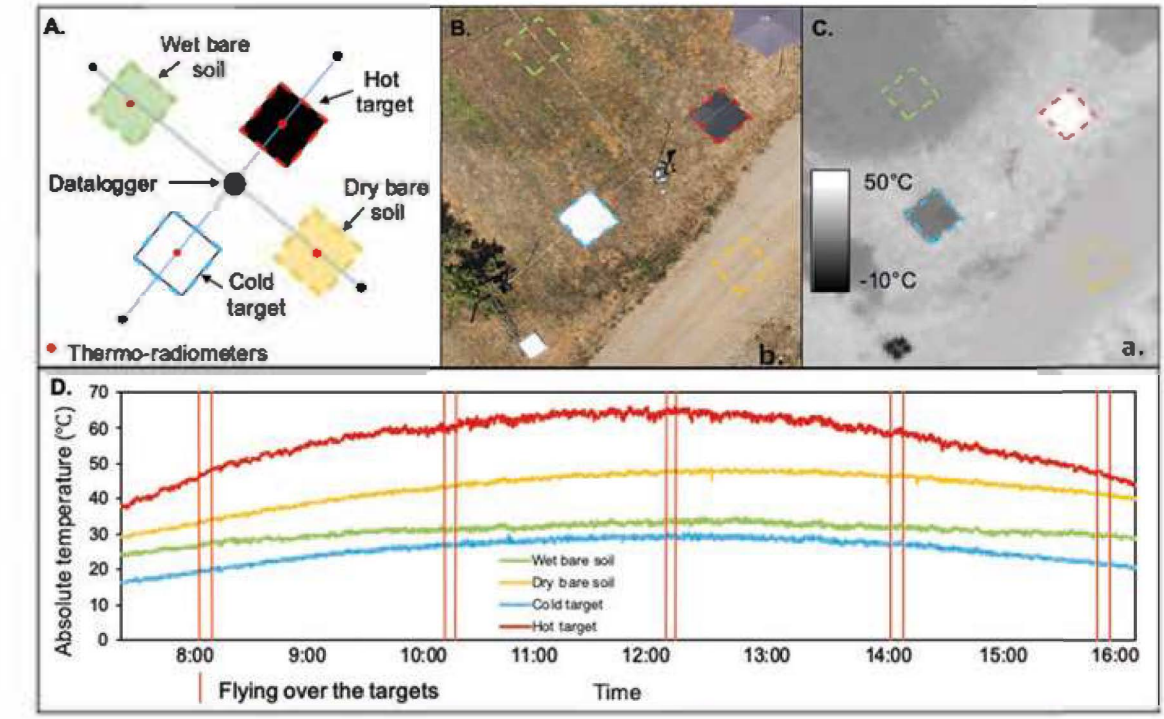

Figure 2.4-5: Thermal targets for radiometric calibration. A.) Schematic drawing of the ground measurements device, B) and C) images of the device in RGB and TIR bands, respectively, D) absolute temperatures recorded over different radiometric targets during UAV flights (adapted from Jolivot et al., 2017, originally published under a CC BY license https://creativecommons.org/licenses/by/4.0/).

angle, circle, square made of piece of metal, black painted panel, wooden board covered with an aluminium film). The TGCPs size will depend on the spatial resolution of the TIR sensor used (usually five to ten-fold larger to ensure their visibility).

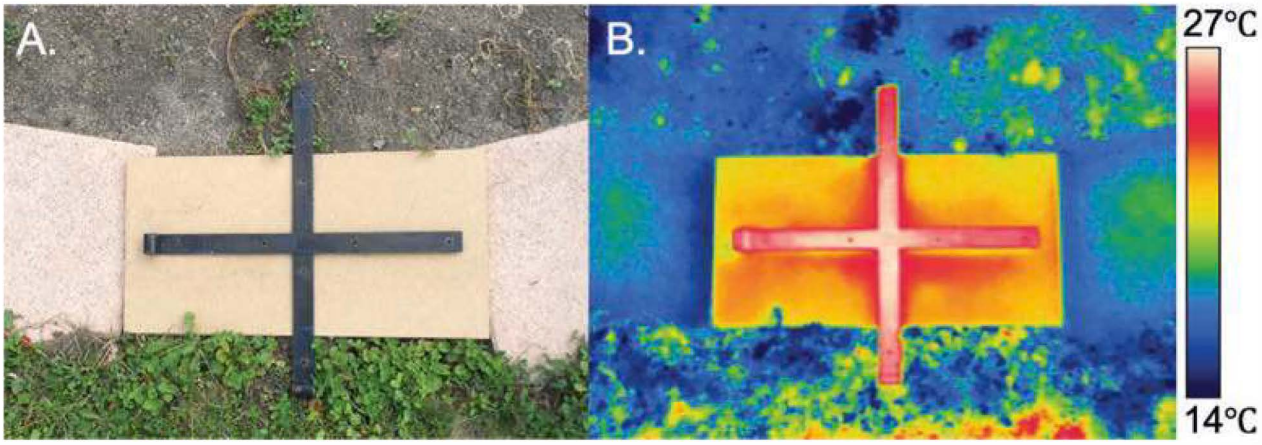

Figure 2.4-6: Geometric thermal target to improve the georeferencing of a TIR map. RGB (A) and TIR (B) images of a thermal target made of a black cross on a wooden board both contrasting with the surroundings in the TIR and RGB bands. ©IRBI – S. Pincebourde. All rights reserved.

Because these patterns are easily identifiable in UAV images in the RGB and in the TIR bands, they can be used for both the RGB and TIR maps geolocation (see detail in Figure 2.4-7).

- Meteorological records and optimal flight conditions
  In order to compare temperature between images or for thermal mapping, weather conditions have to be as stable as possible. Therefore, changes in weather conditions should be monitored to ensure their stability during TIR UAV image acquisition (Faye et al., 2016a). Indeed, changes in weather conditions can have a rapid and adverse impact on the object surface temperature (mainly wind gusts and variations of solar radiation due to cloud passes (Kelly et al., 2019)). Ideally, meteorological data should be recorded using a weather station located nearby the flight area and recording at a fine step-time. The main parameters to monitor are: air temperature and relative humidity, solar and atmospheric radiation, wind speed and direction. Accurate and synchronized time-keeping must be ensured across all devices (dataloggers and TIR camera) and the timer of the GNSS receiver of the UAV. This monitoring allows to confirm that weather conditions were stable during the flights (Figure 2.4-7); if not the acquisition flight should be performed again. Therefore, TIR UAV flights and image acquisition have to be carried out during steady weather conditions, typically full sun periods, with no wind (i.e., gusts below 20 km/h), and no dust or smoke.

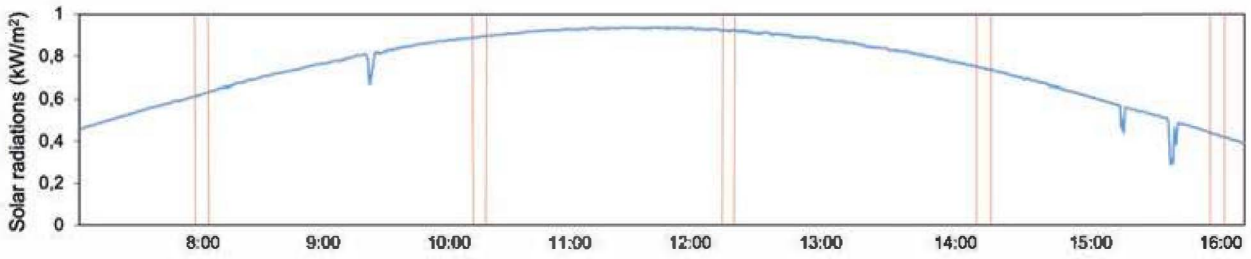

Figure 2.4-7: Solar radiation recorded during a day with clear sky conditions in the south of France in August 2013. The red vertical lines indicate the time of five successive UAV flights. The small peaks below the blue curve are linked to little cloud passes. Unless otherwise stated, all images were prepared by the authors for this chapter.

Moreover, the optimum flight conditions depend on the object of interest and must be established with a thorough knowledge of the studied system. For example, the thermal contrast between the studied object and its surroundings must be maximal in order to optimize the detection of endothermic animals (e.g., flying during night to detect endothermic organisms will be more efficient than during the day because this maximizes the difference in thermal radiance between the studied object and its environment). Not all objects have the same physical properties related to the absorption and emission of thermal-infrared radiation (see 2.4.1.). For instance, some targets such as minerals (e.g., rocks) have higher thermal inertia than others such as vegetation. Rocks thus absorb the thermal-infrared radiation more slowly but also re-emit it more slowly than the vegetation, causing a higher (e.g., rocks) or lower (e.g., vegetation) lag contrast with the surrounding temperatures.

2.4.2.3 Camera settings and flights planning

First of all, in order to retrieve stable temperature data, the TIR camera needs to pre-heat before flying (i.e., stabilisation time). Ribeiro-Gomes et al., 2017 studied uncooled TIR cameras stability with a blackbody device and showed that, under laboratory conditions, at least 30 minutes of pre-heating are needed to obtain stabilized good quality data (Figure 2.4-8). Then, the emissivity should be set to the emissivity value of the main studied object referring in emissivity table (Rubio, 1997) or by experimentally determining it (Zhang et al., 2016). If various objects of interest with a different emissivity are studied, changes will be made in the post-processing (see 2.4.3). To avoid blurred image acquisition, the focus of the lens has to be set manually to the flight height. Last, as stated in 2.4.1., the ambient temperature has to be set as an input in TIR cameras that dispose of an internal calibration system (Table 2.4-1).

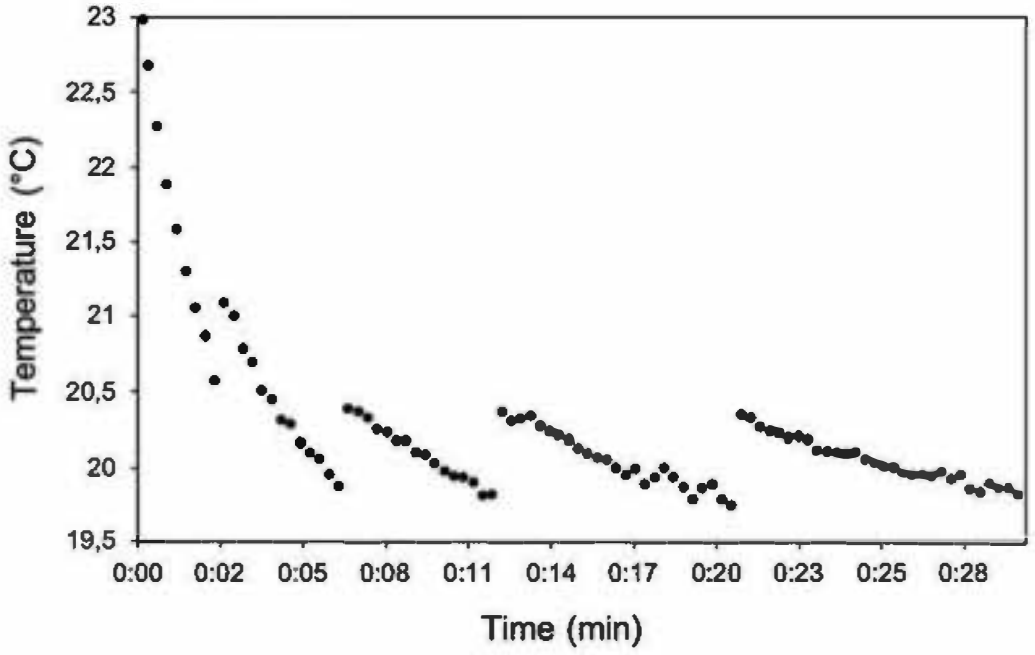

Figure 2.4-8: 30 minutes of temperature readings (Thermotechnix Miricle camera) after switching on the TIR camera. Data acquired each 20 seconds on a blackbody set to 20°C. The jumps correspond to self-calibration events of the TIR camera.

The flight planning for TIR image acquisition is designed in a similar way as for RGB cameras (see chapter 1.5), but it is necessary to consider the lower resolution of the TIR sensor, the shutter speed, and triggering limitations of TIR cameras. Therefore, the flying speed, the elevation, the frontal and side overlap have to be defined considering the TIR camera specifications. TIR ground sampling distance that depends on the pixel size and flying height should be chosen to ensure object detection in the TIR bands. For example, Burke et al., 2019 target a minimum of ten pixels per object (i.e., animal) to ensure effective detection. This aspect must also be taken into account to limit the effects related to mixed pixels (see 2.4.5).

The flight plan should be designed to fly over the radiometric calibration targets as many times as possible per flight (see 2.4.2). This will ensure to achieve a robust calibration relationship and therefore to improve the accuracy of the results. For instance, the UAV can make three passages over the radiometric thermal targets on each flight: at take-off, landing, and once in-between (Figure 2.4-9).

2.4.3 TIR images (pre-)processing

The use of low altitude TIR images acquired by UAV often cannot cover the whole area of interest. It is therefore needed to take a series of images, whereupon images have to be radiometrically corrected, and/or ortho-rectified and mosaicked to map the area of interest. Thermal image processing is a time-consuming step, which must be largely automated before infrared thermography can be applied as a routine tool in environmental practices. The desired temperature accuracy and spatial resolution must be chosen by taking into account the aim of the study.

2.4.3.1 Thermal radiometric corrections

The radiometric corrections can be performed by computing empirical linear equations each time the UAV captured the radiometric thermal targets, depending on flight plan (three times in our example, Figure 2.4-9). The average thermal TIR values for each target (four in the example given in Figure 2.4-5) must be calculated for each image acquired above the targets and then compared to the ground data recorded at exactly the same time by the ground device (Figure 2.4-9). Then, the linear regression equations computed on these temperature data must be applied to the TIR images acquired the closest to the time of the UAV pass over the targets. In our example, the UAV passed three times over the targets and therefore three equations can be computed.

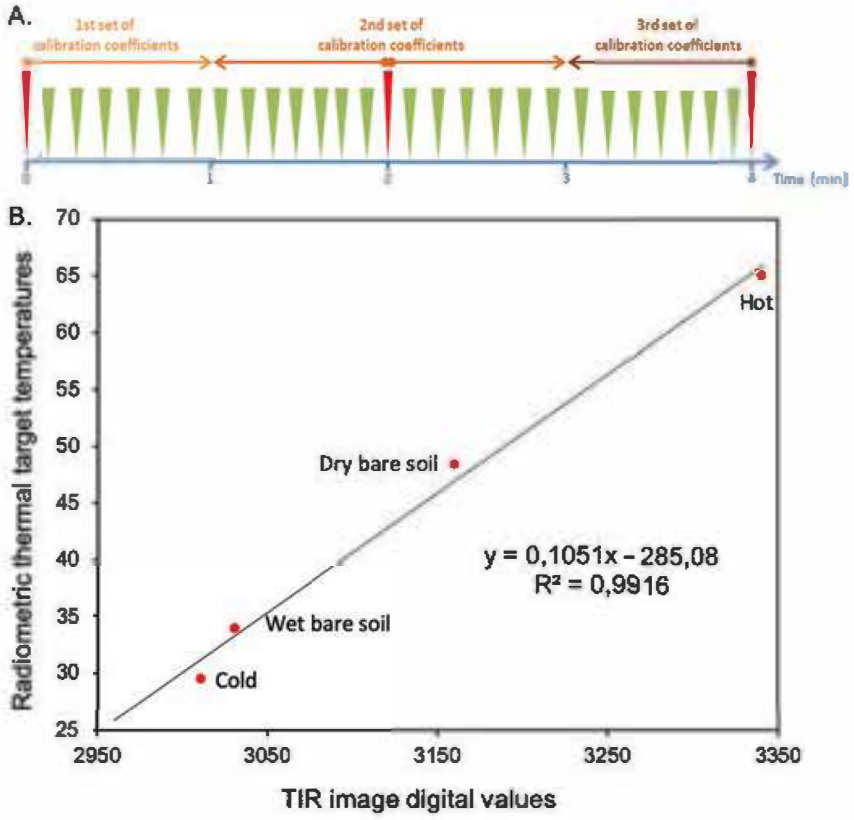

Figure 2.4-9: Radiometric calibration equation applied to retrieve calibrated temperature data. A. green marks on the flight plan represent a single TIR image acquisition and red marks represent TIR images acquired over the thermal calibration targets. B. Example of a ground based TIR imagery radiometric calibration equation for one passage over the thermal targets. Each red dot represents a ground target in Figure 2.4-5. Adapted by permission from Springer Nature Customer Service Centre GmbH: Springer, Precision Agriculture, Gómez-Candón, D., Virlet, N., Labbé, S., Jolivot, A. & Regnard, J. L.: Field phenotyping of water stress at tree scale by UAV-sensed imagery: new insights for thermal acquisition and calibration, © (2016).

Other authors (Salgadoe et al., 2019) made use of non-reference histogram methods for determining average surface temperature, bypassing the procedure based on thermal references.

2.4.3.2 Orthomosaics and geometric corrections using TGCPs

The generation of TIR mapping products can follow the steps presented in chapter 2.2 for RGB orthoimage generation (see examples of a RGB and TIR orthomosaic in Figure 2.4-10). However, the low spatial resolution of the TIR sensor and the low image quality in terms of contrast

and noise, leading to a low signal to noise ratio, make the mosaicking of TIR images less accurate compared to the use of RGB images. One way to improve the accuracy of TIR mapping is to process it in combination with RGB imagery. The RGB images are used to calculate a high-resolution digital elevation model onto which lower resolution TIR images are projected (e.g., Sledz et al., 2018 and Ribeiro-Gomes et al., 2017). This procedure makes it possible to obtain TIR orthomosaics of a much higher quality in term of geometrical correctness.

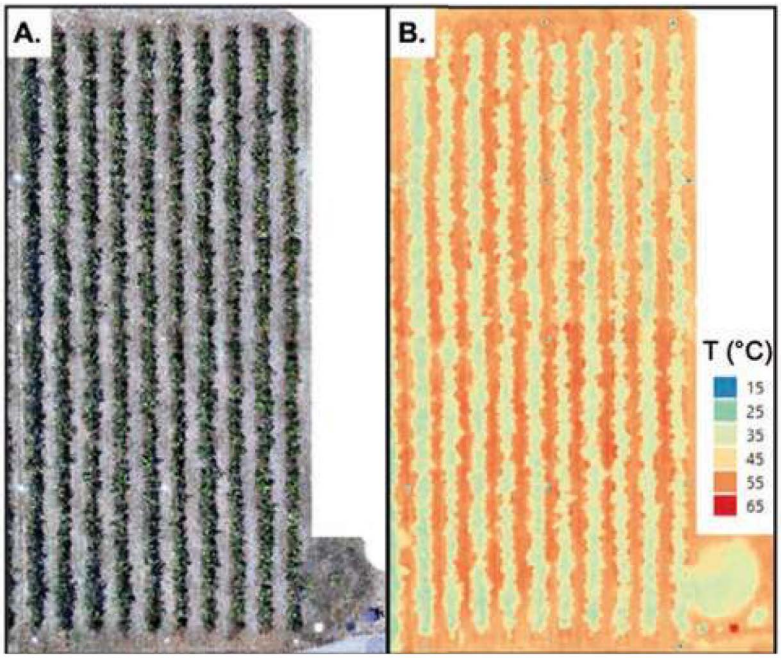

Figure 2.4-10: UAV-based RGB (A) and TIR (B) orthomosaics of a French apple orchard. White and blue dots visible respectively in RGB and TIR orthoimages are the geometric thermal ground control points.

2.4.3.3 Correcting emissivity values for each object in a thermal map

If various objects of interest with different emissivity values are to be studied on the same TIR map (e.g., in order to compare their accurate temperature under the same environmental conditions), Faye et al., 2016a developed a remote sensing procedure bringing together object recognition, masking and cropping objects, with emissivity assignment that can be used to extract object temperature with the appropriate emissivity value. However, by applying this process, Faye et al., 2016a assume that emissivity is spatially and temporally homogeneous for the same object (see Zhang et al., 2016 for details). Moreover, one should be aware that change in emissivity within a 5 % range will only slightly impact the final temperature values (Clark, 1976). Thus, correcting emissivity values of different objects in a TIR map should be made for retrieving

fine-scale discrepancies in absolute temperatures between objects or when studying objects with different values of emissivity (Faye et al., 2016a).

2.4.3.4 Surface temperature cross-validation

Once obtained, the accuracy of temperature in the TIR orthomosaics (radiometrically and emissivity corrected) can be checked. A simple method for temperature quality cross validation consists in comparing temperature values in the corrected TIR image with the temperatures acquired by thermo-radiometers located above artificial targets specifically built for this purpose or placed above natural surfaces already existing in the landscape.

2.4.4 Analyzing TIR images acquired by UAV

2.4.4.1 Relative or absolute surface temperatures

Choosing to work with absolute or relative temperature is an important decision when analysing thermal images. Absolute temperature analysis is justified when comparing image series (e.g., multi-temporal or multi-site) or when an accurate measurement of the temperature of an object is needed.

On the other hand, relative temperature retrieval is suitable to compare thermal data across space (e.g., temperature differences between objects) within the same image or for object detection. Surface temperature excess (i.e., positive or negative deviation between pixel temperature values in the TIR images and ambient air temperature) is a relevant index for direct comparisons of object surfaces' temperature captured under different conditions, regardless of their absolute temperature dissimilarities. But surface temperature excess is sensitive to radiative conditions, wind speed, and vapour pressure deficit (Maes & Steppe, 2012). Temporal comparisons of object responses to environmental conditions based on this index require that ambient conditions are controlled or remain mostly unchanged during experiments (Berger et al., 2010).

2.4.4.2 Image co-registration and data fusion

Coarse resolution of TIR images can be combined with the finer resolution of RGB image, in order to upscale the resolution of the thermal image. A procedure of data fusion, proposed by

Kustas et al. (2003) consists first in regressing thermal pixels of TIR image against an index issued from the high-resolution pixels of the RGB image, this method being feasible only when TIR and RGB images are properly overlaid. Secondly, on the basis of the regression, an estimation of temperature can be obtained for each subpixel, at the finer resolution.

2.4.4.3 Object-based analysis

A category of TIR image analysis focuses on object selection, delineation, and identification based on their spectral (i.e., thermal), shape, and contextual information. This type of analysis can be carried out by photointerpretation or by image processing. Interpretation is done in a similar way to traditional aerial photographs (i.e., *in situ* visual detection made by an observer on board an aircraft). It can also benefit from the motion dimension made possible by acquiring a video data available for some sensors. Recording moving objects in TIR video provides an additional detection feature that is the movement of the target. The detection of moving objects in the video helps the observer to limit the potential confusion between animals and objects (e.g., rocks, stumps). However, photointerpretation remains tedious to perform and is dependent on the observer.

Automatic image analysis allows standardization of the detection approach and the processing of large quantities of images. Whether pixel-based, or object-oriented performed by artificial intelligence-based (e.g., convolutional neural networks), these approaches provide increasing accuracies but remain demanding in terms of parameterization and data availability. Faye et al., 2016a present a workflow to quantify the thermal heterogeneity at the landscape scale based on RGB and TIR maps acquired from UAV and by applying spatial statistics to the TIR values of objects detected and classified using remote sensing technics on the RGB orthoimage.

2.4.4.4 Vegetation indices using the TIR band

The use of thermal image and the spatial variation of surface temperature as a proxy for plant transpiration rate and stomatal conductance is an efficient indicator of the plant water status, because stomatal closure occurs before any other changes in plant water status (Jones, 1992). Thus, TIR imagery provide useful information to monitor plant water status and/or stress using vegetation indices. High precision plant water status maps can be retrieved from remotely sensed TIR imagery through these stress indices, which are very useful tools for irrigation monitoring and plants trait responses to their environment, especially in areas where water resources are limited.

The crop water stress index (CWSI) is one of the most commonly used indices in crop water stress studies and irrigation scheduling applications (Idso et al., 1981). CWSI is a normalized index that was developed to overcome the influence that other environmental variables cause on the relationship between crop temperature and water stress. The empirical CWSI is calculated as:

$$CWSI = \frac{(T_c - T_a) - (T_c - T_a)_{LL}}{(T_c - T_a)_{UL} - (T_c - T_a)_{LL}}$$

where Tc-Ta is the measured difference between canopy and air temperature; $(Tc\text{-}Ta)_{LL}$ is the lower limit of (Tc-Ta) for a given vapor pressure deficit (VPD) which is equivalent to a canopy transpiring at the potential rate; and $(Tc\text{-}Ta)_{UL}$ is the maximum (Tc-Ta), which corresponds to a non-transpiring canopy.

Other commonly used vegetation indices based on TIR imagery are the water deficit index (WDI) (Moran et al., 1994) which is suitable for non-full-cover vegetation surfaces, the temperature-vegetation dryness index (TVDI) that assessess the land-surface dryness (Sandholt et al., 2002), and the vegetation health index (VHI) that combines thermal and multispectral data to monitor vegetation health, drought, and moisture (Choi et al., 2013).

2.4.5 Challenges and limits

By taking into account all the best-practices provided in this chapter to avoid the pitfalls addressed, one should be able to appropriately record accurate thermal data with TIR cameras onboard UAVs in order to address various environmental and other issues. However, some challenges still remain to face in UAVs-borne TIR imagery.

The radiometric correction of the TIR images based on simultaneous ground- and UAV-based thermal recordings with TIR cams is suited to provide accurate surface temperature measurements by taking into account the atmospheric component effects (e.g., distance, particles emission, wind, …) and the potential bias of TIR sensors due to their temperature-dependency (Mesas-Carrascosa et al., 2018). However, even when following this empirical calibration procedure, the resulting accuracies of either calibrated or uncalibrated TIR cameras achieved no less than a few degrees (Yon et al., 2008), a resolution that may not be sufficient for many applications such as ecophysiology or plant phenotyping. Indeed, the ground TIR data that is used for calibration is also affected by the same internal (and to a minor extent external) bias, leading to potential misestimates of absolute surface temperatures. The calibration of TIR sensors against blackbodies is an effective way to increase the accuracy of the TIR measurements (Torres-Rua, 2017), although these materials are not always available, and the procedure is time consuming.

TIR images acquired from UAVs provide instantaneous thermal information spatially distributed, but its associated low-resolution results into difficulties like mixed pixels which affects the interpretation of TIR data (Jones & Sirault, 2014), particularly in heterogeneous surfaces such as plant canopies which do not fully cover the soil. Indeed, when several elements of the study area are included in the same TIR pixel (including part of the studied object), the resulting value of the pixel consists of a temperature mixture of these different elements. In order to avoid misinterpretation of object temperatures due to mixed pixels, we advise to not consider at least two rows of TIR pixels at the border of the studied object and to fly at appropriate elevation to adapt the TIR image resolution at the size of the body object (see 2.4.2.).

Usually, the angle of view when capturing TIR images from a UAV is nadir. But similar to the shooting distance effect (Faye et al., 2016b), the shooting viewing angle is known to impact the TIR cameras readings (Clark, 1976). Thus, care should be taken when analysis temperature readings on TIR images taken with oblique viewing angle. Moreover, these effects might lead to inconsistencies in the TIR orthomosaicking process. As explained by Sledz et al., 2018, the blending step, which identify tie points from several images taken with different viewing angles using the pixels from all parts of the TIR image (including image vignetting effects), is critically hampered by the viewing angle effects, resulting in a lower quality in the TIR orthomosaic reconstruction.

TIR cameras onboard UAVs can provide relatively high-resolution and spatially-resolved surface temperature measurements and, therefore, provide a powerful tool for environmental sciences. But still UAV-TIR measurements provide no information on temperatures of beneath-surface layers (i.e., under canopy, under rock or soil temperatures), which represent a major part of the thermal environment experienced by living organisms. Other thermal approaches, such as proxidetection TIR imaging or punctual thermal recording, can then complement the surface data.

References for further reading

Faye, E., Rebaudo, F., Yánez-Cajo, D., Cauvy-Fraunié, S. & Dangles, O. (2016a) : A toolbox for studying thermal heterogeneity across spatial scales: from unmanned aerial vehicle imagery to landscape metrics, in: Methods in Ecology and Evolution, 7, 437–446.

Gómez-Candón, D., Virlet, N., Labbé, S., Jolivot, A. & Regnard, J. L. (2016) : Field phenotyping of water stress at tree scale by UAV-sensed imagery: new insights for thermal acquisition and calibration, in: Precision Agriculture, 17, 786–800.

Kelly, J., Kljun, N., Olsson, P., Mihai, L., Liljeblad, B., Weslien, P., Klemedtsson, L. & Eklundh, L. (2019) : Challenges and Best Practices for Deriving Temperature Data from an Uncalibrated UAV Thermal Infrared Camera, in: Remote Sensing, 11, 567.

Ribeiro-Gomes, K., Hernández-López, D., Ortega, J., Ballesteros, R., Poblete, T. & Moreno, M. (2017): Uncooled Thermal Camera Calibration and Optimization of the Photogrammetry Process for UAV Applications in Agriculture, in: Sensors, 17, 2173.

Still, C., Powell, R., Aubrecht, D., Kim, Y., Helliker, B., Roberts, D. & Goulden, M. (2019): Thermal imaging in plant and ecosystem ecology: applications and challenges, in: Ecosphere, 10(6).